

Tri-State Cuk Inverter with Power Decoupling for Photovoltaic Applications

Ahmed Darwish^{1*}, Saud Alotaibi¹, and Mohamed A. Elgenedy²

¹Lancaster University, Department of Engineering, Lancaster, United Kingdom

²University of Strathclyde, Electrical and Electronic Engineering Department, Glasgow, United Kingdom

*a.badawy@lancaster.ac.uk

Keywords: Modular DC/AC Inverter, Cuk converter, Photovoltaic applications.

Abstract

This paper proposes modified modulation and control schemes for power decoupling of single-stage single-phase Cuk inverter in continuous conduction mode. Because it has inherent two inductors at the input and output side, the Cuk inverter is able to step up/down the voltage with reduced input and output current ripples. Thus, smaller filtering capacitance, especially at the input side, can be used which increases its suitability for photovoltaic applications. For the maximum power point tracking control, the oscillating even order harmonic components should be eliminated from the inverter's input side otherwise the maximum power cannot be extracted. The proposed modulation scheme will ease the control of inverter's input and output sides. Therefore, the 2nd order harmonic in the input current can be eliminated without adding new active semiconductor switches. In addition, the paper presents a control scheme using fractional-order repetitive control with a conventional proportional-resonant controller. With this closed-loop controller, a sinusoidal output grid current can be generated and controlled while the input current is kept constant with time.

1 Introduction

The fast growth of distributed generation (DG) systems creates a promising opportunity for more dependency on renewable energy systems (RESs) to reduce the global warming threats [1]. Moreover, DG systems improve the electrical power quality and can play an important role in increasing the efficiency and the reliability of the networks [2]. In such decentralised systems, module integrated converters (MICs) are usually employed to convert the input dc voltage and current to ac components and inject the generated current into the local grid [3]. Therefore, reducing the size and increasing the efficiency of these MICs are crucial for the RESs development. Among many inverter topologies, the Cuk inverter has been used in RESs for many reasons. The Cuk converter is current-sourced at both input and output sides and therefore it can reduce the required filtering elements. For other voltage-sourced converters, such as the conventional buck voltage-source inverter (VSI), a large capacitor is required at the input side to filter the input current (output of the RE source) in order to make it suitable for RESs especially photovoltaic (PV) systems. As shown in the typical PV curve in Fig. 1a, the input current should be constant with time in order to achieve the maximum point tracking (MPPT) operation.

The Cuk dc/dc converter, and its ac inverter descendants, can generate output voltages higher or lower than the input voltages and hence they provide more flexibility for the control scheme. Also, the Cuk converter is suitable for isolation with small-size high-frequency transformers (HFTs) which gives an additional ability for voltage boosting, helps to eliminate the electro-magnetic interference (EMI) and grounding issues, and allows for modular configurations as shown in Fig. 1b.

Because of the aforementioned features, several ac descendants for the Cuk converter have been proposed in the literature as three-phase inverters or rectifiers [4]-[5] and single-phase inverters [6]-[8]. The published single-phase Cuk inverters can be categorized into three main types. The first is the differential Cuk inverter as presented in [6] and [9], the second is the unfolding-type Cuk inverter which has been proposed in [7], and the third is the bridgeless Cuk inverter proposed in [8]. In all these types, only one switch is responsible for generating the output voltage/current. Therefore, it is only possible to control either the output or the input sides. Usually, the output side voltage/current is controlled while the input side is left uncontrolled. Because of the oscillating power nature in ac single-phase operation, the input current will be composed of a dc plus a 2nd order harmonic component if only the output side is controlled. It is can be deduced from Fig. 1a that the operational points with the time-variant input currents will be oscillating between the points 2 and 3 of the PV curve. This causes the power to be oscillating between points 4 and 3 which prevents the MPPT from achieving the maximum power and increases the temperature of the PV module, and decrease its lifetime [10]-[14].

In this paper, the Pulse-width Modulation (PWM) of the Cuk inverter in Fig. 2 has been modified in order to employ the output bridge's switches in the current shaping and not only as directors. Thus, an additional degree of freedom is created and the inverter operates as a tri-state Cuk (TS-Cuk) inverter in order to control both input and output sides. In this way, the TS-Cuk inverter will be able to generate ac output voltage and current at 50/60 Hz while keeping the input current constant with time for the MPPT operation.

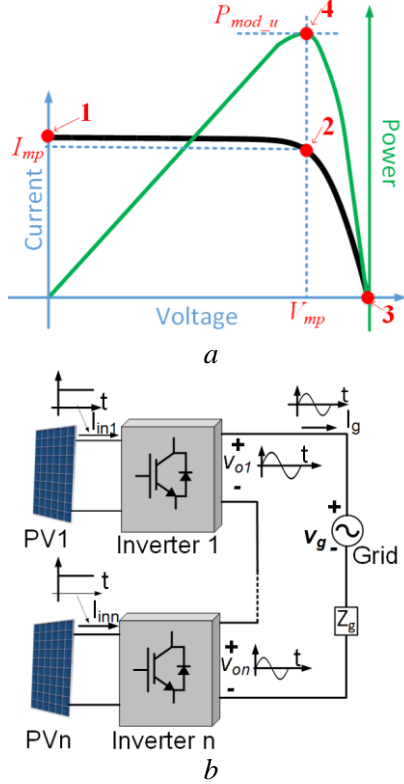


Fig. 1. Grid-connected PV system: (a) I-V curve and (b) Modular configuration

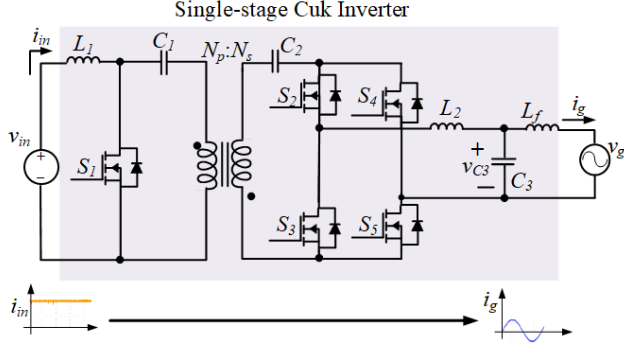


Fig. 2. The proposed TS-Cuk inverter.

2 Inverter's operation

It will be assumed that the inductors L_1 and L_2 are large and hence the inverter operates in CCM. The inverter's switches $S_1 \rightarrow S_5$ have antiparallel diodes $D_1 \rightarrow D_5$.

2.1 Modulation scheme

The operation of the TS-Cuk inverter can be classified into three modes. Assuming that the grid current (i_g) is positive, the inverter's operation during one switching cycle (t_s) can be explained as:

- In the first mode (M_I : $0 \leq t < t_{off}$), S_1 is turned OFF while one of the switches S_2 or S_5 is ON. The input current i_{in} decreases and flows through C_1 which stores energy, see Fig. 3a and Fig. 4. The current (i_o) flows through D_3, S_5 , (or D_4 and

S_2), L_2 and C_3 causing i_g to decrease. When i_g is negative, i_o flows through S_3 and D_5 (or D_2 and S_4) while the input side remains the same. Only one switch is ON in this mode.

- In the second mode (M_{II} : $t_{off} \leq t < t_{off} + t_1$), i_{in} flows through S_1 leading L_1 to store energy. As in Fig. 3b, i_o flows through S_2 and S_5 . Thus, the currents through C_1 and C_2 are reversed leading them to discharge. The energy of C_1 and C_2 transfer to L_2 leading i_o increases. When i_g is negative, i_o flows through S_3 and S_4 while the input side remains the same.

- In the third mode (M_{III} : $t_{off} + t_1 \leq t < t_s$), only S_1 is ON therefore i_{in} keeps increasing. As all the switches in the output bridge are turned OFF, i_o flows through freewheeling diodes D_3 and D_4 (or D_3 and D_5 if i_g is negative) leading C_1 and C_2 to store energy while i_o decreases. Unlike the operation in conventional Cuk converter and its inverter descendants where i_{in} and i_o decrease and increase together, i_o decreases in this mode while i_{in} increases. Thus, this mode decouples the input and output currents behaviors and therefore eliminating the 2nd order harmonic current from the input will be possible. The theoretical waveforms of the proposed TS-Cuk inverter are shown in Fig. 4.

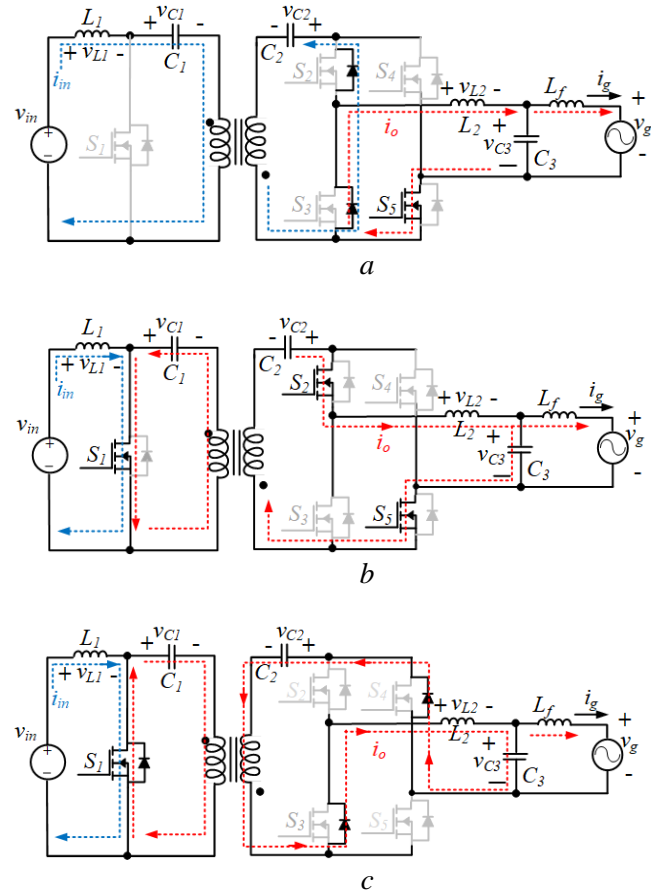


Fig. 3. Operating modes of the Cuk inverter. (a) M_I , (b) M_{II} and (c) M_{III}

2.2 System's average model

The three states in modes M_I , M_{II} and M_{III} in Fig. 3 are averaged using the state-space averaging method in [4] and [7] and hence the average model can be driven in (1) where the

state vector $\mathbf{x}(t) = [i_{in}(t) \ v_{C12}(t) \ i_o(t) \ v_{C3}(t) \ i_g(t)]$ and $y(t) = i_g(t)$ is the grid current. The state $v_{C12}(t)$ is $nv_{C1}(t) + v_{C2}(t)$, n is the turns ratio (N_s/N_p), C_{12} is $C_1C_2/(C_1+n^2C_2)$, $d_1(t)$ is the duty cycle ratio of M_2 , $d_2(t)$ is the duty cycle ratio of M_{III} while $D(t)$ is the duty cycle ratio of switch S_1

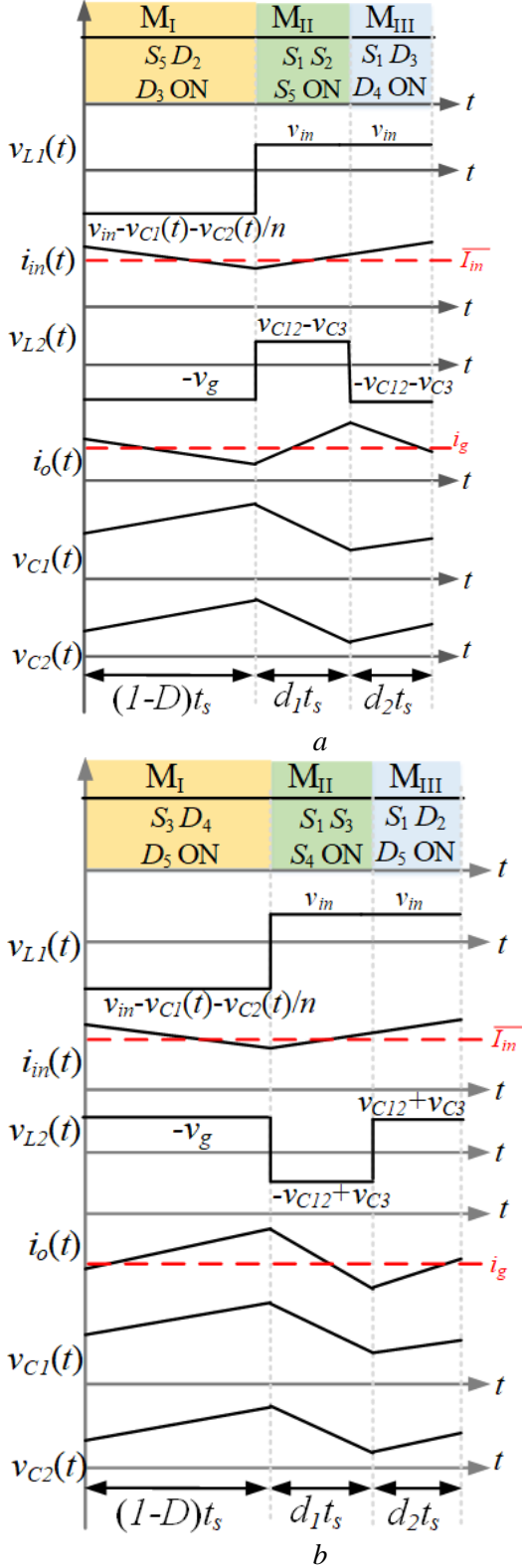


Fig. 4. Theoretical waveforms of the Cuk inverter. (a) positive half cycle and (b) negative half cycle

$$\dot{\mathbf{x}}(t) = \begin{bmatrix} 0 & \frac{D-1}{nL_1} & 0 & 0 & 0 \\ \frac{1-D}{nC_{12}} & 0 & \frac{d_2-d_1}{nC_{12}} & 0 & 0 \\ 0 & \frac{d_1-d_2}{L_2} & 0 & \frac{-1}{L_2} & 0 \\ 0 & 0 & \frac{1}{C_3} & 0 & \frac{-1}{C_3} \\ 0 & 0 & 0 & \frac{1}{L_f} & 0 \end{bmatrix} \mathbf{x}(t) \quad (1)$$

$$+ \begin{bmatrix} \frac{1}{L_1} & 0 \\ 0 & 0 \\ 0 & 0 \\ 0 & 0 \\ 0 & \frac{-1}{L_f} \end{bmatrix} \begin{bmatrix} v_{in} \\ v_g \end{bmatrix}$$

$$y(t) = [0 \ 0 \ 0 \ 0 \ 1] \mathbf{x}(t) \quad (2)$$

The duty cycle ratios can be calculated from Fig. 5 as:

$$d_1 = \frac{t_1}{t_s}, d_2 = \frac{t_2}{t_s} \text{ and } D = d_1 + d_2 \quad (3)$$

The instantaneous power injected to the grid (P_{grid}) is:

$$P_{grid} = v_g(t) i_g(t) \quad (4)$$

If $v_g(t)$ and $i_g(t)$ are expressed as $V_g \sin(\omega t)$ and $I_g \sin(\omega t - \gamma)$, then the grid power is obtained from:

$$P_{grid} = P_{dc} + P_{ac}(t) \quad (5a)$$

$$P_{dc} = \frac{V_g I_g \cos(\gamma)}{2} \quad (5b)$$

$$P_{ac} = \frac{V_g I_g \sin(2\omega t - \gamma - \frac{\pi}{2})}{2} \quad (5c)$$

Because of the additional mode M_{III} and its new control element d_2 , the voltage $v_{C12}(t)$ can be controlled and hence play an important role to remove the 2nd order harmonic from $i_{in}(t)$. To achieve that, the ac power component P_{ac} should be generated from the inside the inverter as:

$$P_{ac} + C_{12} v_{C12}(t) \frac{dv_{C12}(t)}{dt} = 0 \quad (6)$$

$$C_{12} v_{C12}(t) \frac{dv_{C12}(t)}{dt} = -P_{ac} = \frac{V_g I_g \cos(2\omega t - \gamma)}{2}$$

It can be noticed from the (6) that $v_{C12}(t)$ should have dc and ac components and therefore can be assumed as:

$$v_{C12}(t) = V_{dc} + V_{cac} \sin(2\omega t + \varphi) \quad (7)$$

The components V_{dc} and V_{cac} can be found from solving (6) and (7) as:

$$\varphi = \tan^{-1} \left(\frac{\omega L_2 I_g \cos 2\gamma - V_g \sin 2\gamma}{V_g \cos 2\gamma + \omega L_2 I_g \sin 2\gamma} \right) \quad (8)$$

$$V_{cac} = \left(\frac{V_g I_g \cos(2\gamma) + \omega L_2 I_g^2 \cos(2\gamma)}{4\omega C_{12} V_{dc} \cos\varphi} \right)$$

If the capacitors voltage v_{c12} is generated as in (7), the 2nd order current will be eliminated from the input side. To calculate the duty-cycle ratios for achieving that, the first row of the state-space representation in (1) can be written as:

$$\frac{di_{in}(t)}{dt} = \frac{D(t) - 1}{nL_1} v_{c12}(t) + \frac{1}{L_1} v_{in} \quad (9)$$

If it is desired to make $i_{in}(t)$ constant with time, so (9) can be rewritten as:

$$0 = \frac{D(t) - 1}{nL_1} v_{c12}(t) + \frac{1}{L_1} v_{in} \quad (10)$$

$$D(t) = \frac{v_{c12}(t) - nv_{in}}{v_{c12}(t)}$$

Similarly, the third row of (1) can be written as:

$$\frac{di_o(t)}{dt} = \frac{1 - D(t)}{L_2} v_{c12}(t) - \frac{d_2(t) - d_1(t)}{L_2} v_{c3}(t) \quad (11)$$

Arranging (11) and solving for $d_1(t)$ yields:

$$d_1(t) = \frac{L_2 di_o(t)/dt}{2v_{c12}(t)} + \frac{v_{c3}(t)}{2v_{c12}(t)} + \frac{D(t)}{2} \quad (12a)$$

$$d_2(t) = D(t) - d_1(t) \quad (12b)$$

The calculated duty ratios from (12) can be fed-forward assuming that $i_o \approx i_g$ and $v_{c3} \approx v_g$ which are known.

3 Results

The TS-Cuk inverter performance will be illustrated in two ways. The first is when a single module is connected to a single input voltage source V_{in} while the second is when more than one inverter is connected in modular structure as shown in Fig. 1b. Fig. 5 shows the experimental prototype used in this section.

3.1 Single Cuk Inverter

The system is controlled by TMS32028335 DSP and uses the parameters in Table I to keep the voltage and current ripples within 10% of the nominal values. The steps to choose these parameters are well-established in literature [4]-[8] and will be

followed in this paper. The normal power for the inverter in this experiment is 250W and the absolute allowed power is 500W so the controller will be designed assuming that the maximum power is $\tilde{P}_{grid} = 1$ kW, maximum input voltage is $\tilde{V}_{in} = 250$ V and the sum of the capacitors voltage \tilde{V}_{c12} is obtained from (7) as 900 V and the maximum duty cycle ratio can be obtained from (12) as $\tilde{D} = 0.72$, $\tilde{d}_1 = 0.6$ and $\tilde{d}_2 = 0.12$. Assuming an inverter's efficiency of 90% the input current will not exceed $\tilde{I}_{in} = 15$ A.

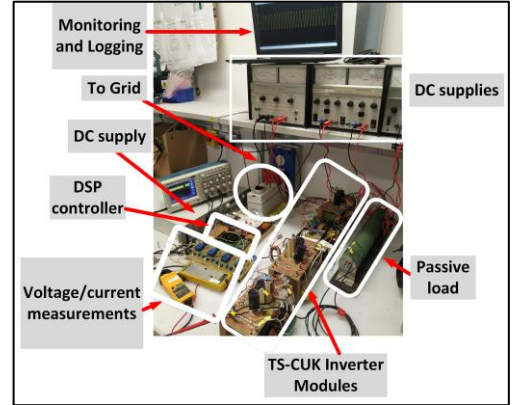


Fig. 5. Experimental setup

Table 1 Parameters of the Cuk inverter

Symbol	Parameter	Value
P_{grid}	Grid power (one Cuk module)	250 W
V_{in}	Nominal input voltage	50 V
V_g	Grid voltage (Trans. primary peak)	200 V
f	Grid frequency	50 Hz
f_s	Switching frequency	50 kHz
$C_1 - C_2$	Cuk middle capacitors	100 μ F
$L_1 - L_2$	Cuk inductors	1 mH
$R_{L1} - R_{L2}$	resistances of L_1 & L_2	0.2 Ω
C_3	Cuk output capacitor	10 μ F
L_f	transformer's inductance	0.1 mH
n	Transformer turns' ratio	1
$S_1 - S_5$	Semiconductor switch	IRG4PC50FPbF
$D_1 - D_5$	Diode	FFSH40120ADN

Fig. 6 shows the results of the TS-Cuk inverter when it injects 250 W in the local ac grid at unity power factor. Fig. 6a shows the input current where the 2nd order harmonic component has been completely eliminated. Fig. 6b shows the capacitors C_1

and C_2 voltages where the 2nd order oscillating power is stored temporarily in these capacitors. The grid voltage and current are shown in Fig. 6c. Fig. 6d shows the THD values of i_g with different loadings.

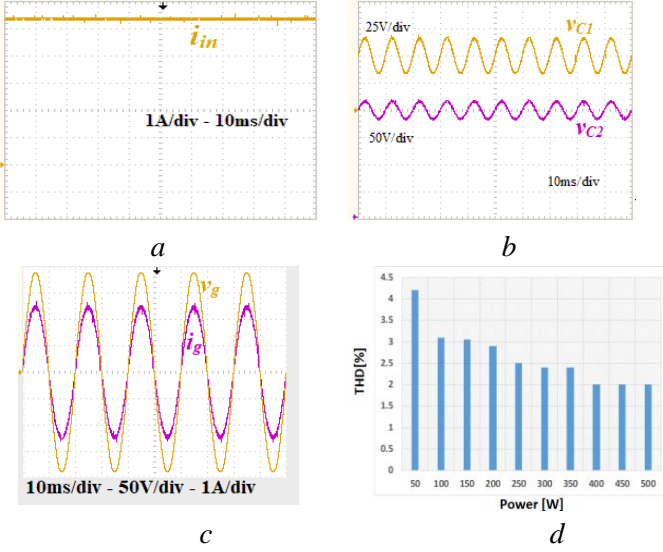


Fig. 7. Experimental results: (a) input current, (b) capacitors voltages, (c) output voltage/current and (d) THD of i_g

3.2 Series Connection and Partial Shading

It has been shown in [3] that the series-connected modular structure, shown in Fig. 1b, can improve the performance of the grid-connected PV systems when operating at higher power levels due to the reduced voltage and current stresses, lower power losses, redundancy and scalability. The TS-Cuk inverter is suitable for this application as the isolating transformer and output bridge will prevent any circulating currents from commutating between the modules. A PV module is expected to reduce its maximum power point during partial shading conditions as shown from the I-V and P-V characteristics in Fig. 7a. Although the characteristics of the PV modules vary with their type and connection, the P-V curve will always have reduced peak values in shading conditions. In such conditions, the current reference $R(t)$ for the shaded modules should be changed in order to extract the maximum available power from all PV modules. The current reference during normal conditions when all modules share the same power is calculated as:

$$R(t) = i_g(t) = \frac{N[v_{C3}(t)] - v_g(t)}{X_{Lf}} = \frac{N[V_o \sin(\omega t + \theta)] - v_g(t)}{X_{Lf}} \quad (13)$$

where N is the number of modules and V_o is the peak value of v_{C3} in normal conditions. If the cables losses are neglected, the total output power in normal conditions is calculated from:

$$P_{total} = \frac{NV_o I_g \cos(\theta - \gamma)}{2} \approx \frac{V_g I_g \cos(\theta - \gamma)}{2} \quad (14)$$

The power of each module is calculated from:

$$P_{mod_u} = V_{in} I_{in} = \frac{V_o I_g \cos(\theta - \gamma)}{2} \approx \frac{V_g I_g \cos(\gamma)}{2N} \quad (15)$$

Thus, at the normal condition when each module can produce power = P_{mod_u} , the reference current is calculated from (13) and the output voltages of the modules are obtained from (15). When some of the modules are shaded as shown in Fig. 7a, the new grid current becomes:

$$i_g(t) = \frac{(N - k)[V_o \sin(\omega t + \theta)] + kV_{sh} \sin(\omega t + \theta_{sh}) - v_g(t)}{X_{Lf}} = \dot{I}_g \sin(\omega t - \gamma) \quad (16)$$

where k is the number of the shaded modules, $i_g(t)$ is the new grid current in order to harvest the maximum available power from shaded and unshaded modules, V_{sh} is the peak value of v_{C3} of the shaded modules. The extracted power from the shaded modules is:

$$P_{mod_sh} = V_{in_sh} I_{in_sh} = \frac{V_{o_sh} \dot{I}_g \cos(\theta_{sh} - \gamma)}{2} \quad (17)$$

The total power harvested from the system becomes:

$$P_{total} = kV_{in_sh} I_{in_sh} + (N - k)V_{in} I_{in} = \frac{(N - k)V_o \dot{I}_g \cos(\theta - \gamma) + kV_{o_sh} \dot{I}_g \cos(\theta_{sh} - \gamma)}{2} \approx \frac{V_g \dot{I}_g \cos(\gamma)}{N} \quad (18)$$

If P_{mod_sh} , V_{in_sh} and I_{in_sh} are known from the PV module offline data or online characteristics calculations, the new current $i_g(t)$ and the unshaded output voltage of the shaded Cuk modules can be amended according to (16), (17) and (18) in order to operate the N modules at the peaks of their P-V curves. To simulate this operation, an experimental case study is carried out with four Cuk inverter modules ($N=4$) connected as shown in Fig. 1b. The system is connected to the grid without voltage reduction as $V_g = 324V$. In the normal unshaded condition before the shading moment t_{sh} , the system supplies 1 kW to the grid and each module generates 250W. At the shading time t_{sh} , the power of the third and fourth modules drops to 20% while the first and second modules' powers remain unchanged. Fig. 7b and 7c show i_{in} and v_{in} for the first (unshaded) and the fourth (shaded) modules. Fig. 7d shows the output voltages v_{C3} of the first and fourth modules. The secondary side capacitor voltages v_{C2} of the first and fourth modules are shown in Fig. 7e. Finally, the grid voltage with current is shown in Fig. 7f. In this case, the new reference current is calculated from (16) in order to extract 50W of the shaded modules while keeping the unshaded modules at 250W. As shown from Fig. 7d, the voltages v_{C3} of unshaded modules increase while they decrease for the shaded modules as per calculated from (16). The resultant power can be

calculated from Fig. 7f as ≈ 600 W which is the maximum assumed power to be available from the input sources.

4 Conclusion

This paper presents a tri-state operation of the single-phase Cuk inverter for PV applications. The proposed TS-Cuk inverter eliminates the even harmonics in the input current without any additional circuits. Thus, the total efficiency of the inverter is higher than its Cuk versions counterparts. The TS-Cuk inverter is suitable for modular configurations when more than inverter is connected in series to reduce the voltage/current stresses and increase the reliability. A generic method has been illustrated to calculate the current references of the inverter to extract the maximum available PV power in shading conditions. The TS-Cuk inverter doubles the PV system's efficiency if it is calculated with respect to the available PV power.

5 References

- [1] M. Mirjafari, S. Harb and R. S. Balog, "Multiobjective Optimization and Topology Selection for a Module-Integrated Inverter," in *IEEE Transactions on Power Electronics*, vol. 30, no. 8, pp. 4219-4231, Aug. 2015
- [2] "Solar micro inverter - Global market outlook (2017-2023)," Statistics Market Research Consulting Pvt Ltd, Gaithersburg, MD, USA, Rep., Jun. 2013.
- [3] L. Zhang, K. Sun, Y. W. Li, X. Lu and J. Zhao, "A Distributed Power Control of Series-Connected Module-Integrated Inverters for PV Grid-Tied Applications," in *IEEE Transactions on Power Electronics*, vol. 33, no. 9, pp. 7698-7707, Sept. 2018.
- [4] A. Darwish, A. M. Massoud, D. Holliday, S. Ahmed and B. W. Williams, "Single-Stage Three-Phase Differential-Mode Buck-Boost Inverters with Continuous Input Current for PV Applications," in *IEEE Trans. on Power Electro.*, vol. 31, no. 12, pp. 8218-8236, Dec. 2016.
- [5] J. Kikuchi and T. A. Lipo, "Three-phase PWM boost-buck rectifiers with power-regenerating capability," in *IEEE Transactions on Industry Applications*, vol. 38, no. 5, pp. 1361-1369, Sept.-Oct. 2002
- [6] S. Mehrnami and S. K. Mazumder, "Discontinuous modulation scheme for a differential-mode Cuk Inverter," *IEEE Trans. on Power Electron.*, vol. 30, no. 3, pp. 1242-1254, Mar. 2015
- [7] B. Han, J. Lee, M. Kim, "Repetitive controller with phaselead compensation for Cuk CCM inverter," *IEEE Trans. Ind. Electron.*, vol. 65, no. 3, pp. 2356-2367, Mar. 2018.
- [8] B. Han, J. Lai and M. Kim, "Bridgless Cuk-Derived Single Power Conversion Inverter with Reactive Power Capability," in *IEEE Transactions on Power Electronics*. Early Access 2019.
- [9] A. Darwish, A. Massoud, D. Holliday, S. Ahmed and B. Williams, "Generation, performance evaluation and control design of single-phase differential-mode buck-boost current-source inverters," in *IET Renewable Power Generation*, vol. 10, no. 7, pp. 916-927, 7 2016.
- [10] B. N. Alajmi, et. al, "Single-Phase Single-Stage Transformer less Grid-Connected PV System," in *IEEE Trans.on Power Electron.*, vol. 28, no. 6, pp. 2664-2676, June 2013.
- [11] Ahmed Darwish, Saud Alotaibi, and Mohamed A. Elgenedy. "Current-source Single-phase Module Integrated Inverters for PV Grid-connected Applications." *IEEE Access* (2020).
- [12] A. Darwish, A. Elserougi, A. Abdel-Khalik, S. Ahmed, A. Massoud, D. Holliday, and B. Williams, "A single-stage three-phase DC/AC inverter based on Cuk converter for PV application," in *GCC Conference and Exhibition (GCC)*, 2013 7th IEEE, 2013, pp. 384-389
- [13] A. Darwish Badawy, "Current source dc-dc and dc-ac converters with continuous energy flow," Degree of Doctor of Philosophy, Department of Electronics and Electrical Engineering, University of Strathclyde, Glasgow, 2015.

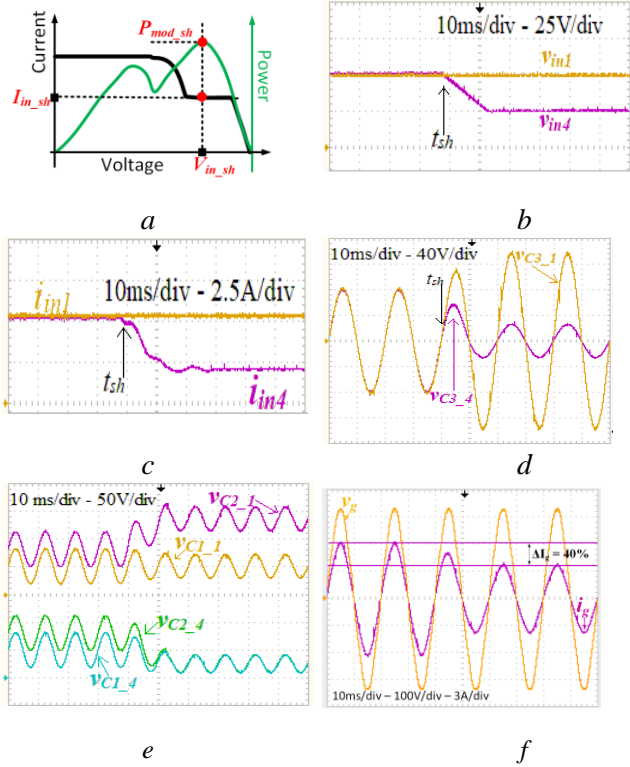


Fig. 7. Partial shading conditions: (a) P-V curve, (b) input voltages, (c) input currents, (d) module's output voltages, (e) capacitors voltages, and (f) grid voltage and current

If one PV module is completely shaded, the inverter associated with this module will generate zero output voltage and can be bypassed by its output switches. So, the unshaded modules' inverters will generate higher voltages to compensate this voltage difference with the grid voltage. A SIMULINK model tests this case shown in Fig. 8 when module no. 4 of the Cuk type system is completely shaded at time $t = 0.1$

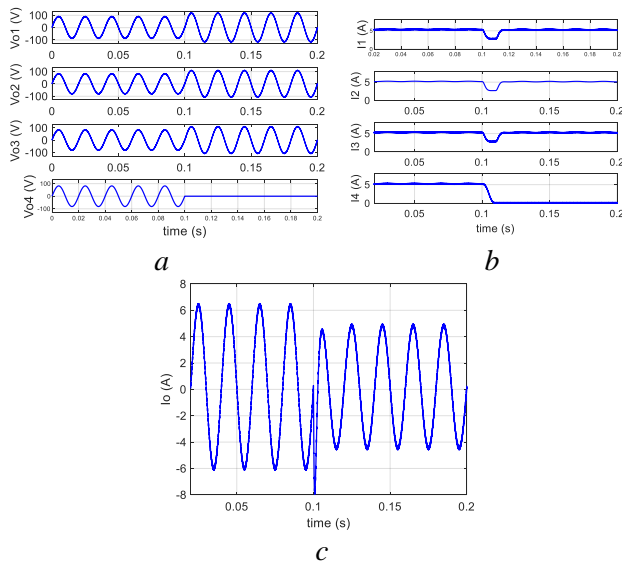


Fig. 8. Cuk inverter's operation when module 4 is completely bypassed: (a) modules' output voltages, (b) input currents and (c) total output current